Closed-Form Direction Finding and Polarization Estimation with Arbitrarily Spaced Electromagnetic Vector-Sensors at Unknown Locations

Kainam Thomas Wong, *Member, IEEE* and Michael D. Zoltowski, *Fellow, IEEE*

***Abstract*—This paper introduces a new closed-form ESPRIT-based algorithm for multisource direction finding and polarization estimation with arbitrarily spaced electromagnetic vector-sensors whose three-dimensional (3-D) locations need *not* be known. The vector-sensor, already commercially available, consists of six colocated but diversely polarized antennas separately measuring all six electromagnetic-field components of an incident wavefield. ESPRIT exploits the nonspatial interrelations among the six unknown electromagnetic-field components of each source and produces from the measured data a set of eigenvalues, from which the source's electromagnetic-field vector may be estimated to within a complex scalar. Application of a vector cross-product operation to this ambiguous electromagnetic-field vector estimate produces an unambiguous estimate of that source's normalized Poynting vector, which contains as its components the source's Cartesian direction cosines. Monte Carlo simulation results verify the efficacy and versatility of this innovative scheme. This novel method maybe considered as a simplification and a refinement over Li's earlier work in 1993 [8].**

***Index Terms*—Array signal processing, direction of arrival estimation, intelligent sensors, navigation, polarization, radar signal processing, radio direction finding, signal processing antennas.**

I. Introduction

ESTIMATION of signal parameters via rotational invariance techniques (ESPRIT [3]) represents a highly popular eigenstructure (subspace) based parameter estimation method. Eigenstructure (subspace) based methods are so labeled because they decompose the column space of the data correlation matrix into a signal subspace and a noise subspace. ESPRIT requires a certain invariance structure in the sampled data set; and this invariance structure has generally been realized in most ESPRIT-based direction finding (DF) algorithms as a *spatial* invariance dependent on some known translational displacement (Δ) between two identical subarrays of sensors. In contrast, this proposed algorithm advances a nonspatial realization of ESPRIT's invariance structure such that the invariance factors depend only on the impinging signals' direction cosines but not on array geometry. This proposed algorithm also offers closed-form solutions for any irregular and even possibly unknown array geometry, whereas most other algorithms would require iterative searches (such as the MUSIC algorithm [1]) to handle arbitrary and *a priori* known array geometry.[1] Hence, this proposed algorithm: 1) is computationally less intensive than many open-form search methods; 2) requires no *a priori* coarse estimates of the arrival angle to start off any iterative search; and 3) makes possible sparse array aperture extension while producing closed-form unambiguous arrival angle estimation with no extra computation needed for disambiguation. Because this novel algorithm is also highly parallel in its computational structure, concurrent computer processing facilitates real-time implementations. All these innovations are realized by the creative use of electromagnetic vector-sensors as explained below.

This novel scheme employs electromagnetic vector-sensors, each of which consists of six spatially colocated but diversely polarized antennas, separately measuring all three electrical-field components and all three magnetic-field components of the incident wave field. Electromagnetic vector-sensors can exploit any polarization diversity among the impinging radar sources [17]. Electromagnetic vector-sensors are already commercially available, for example, from Flam and Russell, Inc., Horsham, PA [4], [6], and from EMC Baden, Inc., Baden, Switzerland.

Diversely polarized antenna arrays have been exploited in a number of direction finding algorithms that extend the direction finding approach used for spatially displaced uniformly polarized antenna arrays. These works, however, often use only dipole pairs or dipole triads and thus can extract information only of two or three electric field components out of all six electromagnetic field components. The first direction finding algorithms explicitly exploiting all six electromagnetic components appear to have been developed separately by Nehorai and Paldi [5], [14] and Li [8]. Nehorai and Paldi [5], [14], who coined the term "vector-sensor," pioneered the simple but novel idea of using the vector cross-product of the electric field vector estimate and the magnetic field vector estimate (provided the electromagnetic vector-sensor outputs) to estimate directly the two-dimensional radial direction of a source. Their seminal paper also proposes a scalar performance

Manuscript received May 25, 1997; revised October 21, 1999. This work was supported by the U.S. National Science Foundation under Grant MIPS-9320890, the U.S. Air Force Office of Scientific Research under Contract F49620-95-1-0367, and the U.S. Army Research Office Focused Research Initiative under Grant DAAH04-95-1-0246.

K. T. Wong is with the Department of Electronic Engineering, Chinese University of Hong Kong, Shatin, NT, Hong Kong (e-mail: ktwong@ieee.org).

M. D. Zoltowski is with School of Electrical and Computer Engineering, Purdue University, West Lafayette, IN 47907-1285 USA (e-mail: mikedz@ecn.purdue.edu).

Publisher Item Identifier S 0018-926X(00)03268-3.

[1]The basic algorithm herein proposed requires all vector-sensors to have an identical and known orientation; however, a calibration and correction procedure is also proposed to handle the case where individual vector-sensors are diversely oriented in an arbitrary and unknown manner. A possible scenario where the vector-sensors may have unknown array spacing but identical orientation may be in a battlefield situation where individual mobile vector-sensor units are set up at *ad hoc* locations but soldiers are equipped with instruments to correctly orient each unit.

measure, the mean square angular error (MSAE), and derives an expression and a bound for the MSAE for the vector-sensor. That same paper also proposes using one electromagnetic vector-sensor to estimate the DOA's, but not by eigenstructure methods as herein proposed. The vector cross-product estimator was first adapted to *ESPRIT* by Wong and Zoltowski [20], [22], [31], [32], extending array aperture for regularly spaced vector-sensors without ambiguity in the direction-cosine estimates. Li's method in [8] (to be further discussed in the following paragraph) is extended for partially polarized sources by Ho *et al.* [29]. Burgess and Van Veen [10]–[12] deployed a multiple vector-sensor array for signal detection along specific preset arrival directions and polarization states but did not explore direction finding. Hochwald and Nehorai [13] employed vector-sensors in polarimetric modeling. Hatke [9], Ho *et al.* [16], and Tan *et al.* [19] investigated vector-sensor uniqueness and identifiability issues. Wong and Zoltowski [21] also presented another ESPRIT-based method that estimates the directions-of-arrival of multiple sources using only a single vector-sensor. Wong and Zoltowski [24] also developed another multiple vector-sensor direction finding algorithm that adaptively steers null beams in polarization space using a self-initiating iterative search method that requires no *a priori* source information. Adaptive source tracking is investigated by Nehorai and Tichavsky in [30].

The present paper may be considered as a simplification and a refinement of Li's ESPRIT-based algorithm [8] for magnetic loops and electric dipoles. Like [8] but unlike [20], [22], [23], [31], [32], the present algorithm considers the L electromagnetic vector-sensors (with their $6L$ components) as six colocated subarrays each of which comprises identically polarized antennas but among which the polarization is diverse. Like [8], the present algorithm applies ESPRIT multiple times to distinct pairs of these six subarrays to extract the invariant factors characterizing the six electromagnetic field components of the impinging sources. The pivotal insight of this paper is that five invariant factors[2] relating the six electromagnetic field components suffice for unique determination of the source's normalized Poynting vector and, thus, source's arrival angles. That is, these five invariant factors would produce an ambiguous estimate of each impinging source's electromagnetic field vector, correct to within a complex scalar. This electromagnetic-field vector estimate, though ambiguous, can produce an unambiguous estimate of the source's normalized Poynting vector via a vector cross product. This algorithm thus substitutes the elegant and simple operation of a vector cross product for the complex manipulation in [8] involving a set of highly nonlinear equations. That both the present algorithm and [8] do not require any *a priori* knowledge of the location of any of the vector-sensors is because the aforementioned invariant factors depend only on the source parameters but not on the electromagnetic vector-sensors' spatial locations.

[2]After the camera-ready copy of this manuscript was submitted, the first author recognized that only four invariant factors, not five, need to be evaluated. Please refer to the footnotes in Sections III-A and III-D for explanation.

II. Mathematical Data Model

Uncorrelated transverse electromagnetic plane waves, having traveled through a homogeneous isotropic medium, impinge upon a three-dimensional (3-D) array of arbitrarily spaced but identically oriented electromagnetic vector-sensors at possibly unknown spatial locations. This identical orientation assumption will be relaxed in Section IV. The kth such unit-power completely polarized incident source has the electric-field vector $\boldsymbol{e}_k$ and the magnetic-field vector $\boldsymbol{h}_k$, which may be expressed in Cartesian coordinates as [5], [14] (after accounting for the the transmission medium's intrinsic impedance)

$$\begin{aligned}\boldsymbol{a}(\theta_k,\,\phi_k,\,\gamma_k,\,\eta_k) &\\ \stackrel{\text{def}}{=}\begin{bmatrix}\boldsymbol{e}_k\\ \boldsymbol{h}_k\end{bmatrix} &\stackrel{\text{def}}{=}\begin{bmatrix}e_{x_k}\\ e_{y_k}\\ e_{z_k}\\ h_{x_k}\\ h_{y_k}\\ h_{z_k}\end{bmatrix}\stackrel{\text{def}}{=}\begin{bmatrix}a_1(\theta_k,\,\phi_k,\,\gamma_k,\,\eta_k)\\ a_2(\theta_k,\,\phi_k,\,\gamma_k,\,\eta_k)\\ a_3(\theta_k,\,\phi_k,\,\gamma_k,\,\eta_k)\\ a_4(\theta_k,\,\phi_k,\,\gamma_k,\,\eta_k)\\ a_5(\theta_k,\,\phi_k,\,\gamma_k,\,\eta_k)\\ a_6(\theta_k,\,\phi_k,\,\gamma_k,\,\eta_k)\end{bmatrix}\end{aligned} \tag{1}$$

$$= \underbrace{\begin{bmatrix}\cos\phi_k\cos\theta_k & -\sin\phi_k\\ \sin\phi_k\cos\theta_k & \cos\phi_k\\ -\sin\theta_k & 0\\ -\sin\phi_k & -\cos\phi_k\cos\theta_k\\ \cos\phi_k & -\sin\phi_k\cos\theta_k\\ 0 & \sin\theta_k\end{bmatrix}}_{\stackrel{\text{def}}{=}\boldsymbol{\Theta}(\theta_k,\,\phi_k)} \underbrace{\begin{bmatrix}\sin\gamma_k\,e^{j\eta_k}\\ \cos\gamma_k\end{bmatrix}}_{\stackrel{\text{def}}{=}\boldsymbol{g}_k} \tag{2}$$

where

$0\le\theta_k<\pi$ denotes the signal's elevation angle measured from the vertical z-axis;

$0\le\phi_k<2\pi$ symbolizes the azimuth angle;

$0\le\gamma_k<\pi/2$ represents the auxiliary polarization angle;

$-\pi\le\eta_k<\pi$ signifies the polarization phase difference.

While the above electromagnetic vector-sensor model has not accounted for mutual coupling among the vector-sensor's six component-antennas, this model has been reported by Flam & Russell, Inc. to be a very good approximation of their CART array implementation of the electromagnetic vector-sensor concept.[3] Note also that $\boldsymbol{\Theta}(\theta_k,\,\phi_k)$ depends only on the sources' spatial angular locations and $\boldsymbol{g}_k$ depends only on the incident signals' polarization states. This fact is pivotal to the polarization estimation procedure to be proposed.

$\boldsymbol{e}_k$ and $\boldsymbol{h}_k$ are orthogonal to each other and to the kth source's direction of propagation, i.e., the normalized Poynting-vector $\boldsymbol{p}_k$

$$\boldsymbol{p}_k\stackrel{\text{def}}{=}\begin{bmatrix}p_{x_k}(\theta_k,\phi_k)\\ p_{y_k}(\theta_k,\phi_k)\\ p_{z_k}(\theta_k,\phi_k)\end{bmatrix}=\boldsymbol{e}_k\times\boldsymbol{h}_k^*\stackrel{\text{def}}{=}\begin{bmatrix}u_k\\ v_k\\ w_k\end{bmatrix}=\begin{bmatrix}\sin\theta_k\cos\phi_k\\ \sin\theta_k\sin\phi_k\\ \cos\theta_k\end{bmatrix} \tag{3}$$

[3]"...the patterns of the loops and dipoles [of the CART array] are EXTREMELY close to the theoretical patterns, indicating very good isolation and balance among the elements."*—private correspondence, R. Flam, Flam & Russell, to first author, Jan. 15, 1997.*

where

*	denotes complex conjugation;
$u_k \stackrel{\text{def}}{=} \sin\theta_k \cos\phi_k$	represents the direction-cosine along the x-axis;
$v_k \stackrel{\text{def}}{=} \sin\theta_k \sin\phi_k$	symbolizes the direction-cosine along the y-axis;
$w_k \stackrel{\text{def}}{=} \cos\theta_k$	signifies the direction-cosine along the z-axis.

Note that the three components of the normalized Poynting vector simply correspond to the three direction cosines of the impinging source. This fact is basic to the efficacy of the present algorithm.

The inter-vector-sensor spatial phase factor relating the kth narrow-band[4] point source to the lth electromagnetic vector-sensor at the (possibly unknown) location (x_l, y_l, z_l) is

$$q_l(\theta_k, \phi_k) \stackrel{\text{def}}{=} e^{j2\pi((x_l u_k + y_l v_k + z_l w_k)/\lambda)} = \underbrace{e^{j2\pi(x_l u_k/\lambda)}}_{\stackrel{\text{def}}{=} q_l^x(u_k)} \underbrace{e^{j2\pi(y_l v_k/\lambda)}}_{\stackrel{\text{def}}{=} q_l^y(v_k)} \underbrace{e^{j2\pi(z_l w_k/\lambda)}}_{\stackrel{\text{def}}{=} q_l^z(w_k)}. \quad (4)$$

The $6L \times 1$ array manifold for the entire L-element electromagnetic vector-sensor array is

$$\boldsymbol{a}^{(L)}(\theta_k, \phi_k, \gamma_k, \eta_k) \stackrel{\text{def}}{=} \boldsymbol{a}(\theta_k, \phi_k, \gamma_k, \eta_k) \otimes \underbrace{\begin{bmatrix} q_1(\theta_k, \phi_k) \\ \vdots \\ q_L(\theta_k, \phi_k) \end{bmatrix}}_{\stackrel{\text{def}}{=} \boldsymbol{q}(\theta_k, \phi_k) = \boldsymbol{q}(u_k, v_k)} \quad (5)$$

where $\otimes$ symbolizes the Kronecker-product operator. With a total of $K \leq L$ cochannel signals, the entire array would yield a $6L \times 1$ vector measurement $\boldsymbol{z}(t)$ at times t

$$\boldsymbol{z}(t) = \sum_{k=1}^{K} \boldsymbol{a}^{(L)}(\theta_k, \phi_k, \gamma_k, \eta_k) s_k(t) + \boldsymbol{n}(t) = \boldsymbol{A}\boldsymbol{s}(t) + \boldsymbol{n}(t) \quad (6)$$

where

$$s_k(t) \stackrel{\text{def}}{=} \sqrt{\mathcal{P}_k}\sigma_k(t) e^{j(2\pi(c/\lambda)t + \varphi_k)} \quad (7)$$

$$\boldsymbol{A} \stackrel{\text{def}}{=} \left[\boldsymbol{a}^{(L)}(\theta_1, \phi_1, \gamma_1, \eta_1), \cdots, \boldsymbol{a}^{(L)}(\theta_K, \phi_K, \gamma_K, \eta_K)\right] \quad (8)$$

$$\boldsymbol{s}(t) \stackrel{\text{def}}{=} \begin{bmatrix} s_1(t) \\ \vdots \\ s_K(t) \end{bmatrix}; \qquad \boldsymbol{n}(t) \stackrel{\text{def}}{=} \begin{bmatrix} n_1(t) \\ \vdots \\ n_{6L}(t) \end{bmatrix} \quad (9)$$

and $\boldsymbol{n}(t)$ symbolizes the $6L \times 1$ additive complex-valued zero-mean white noise vector, $\mathcal{P}_k$ denotes the kth signal's power, $\sigma_k(t)$ represents a zero-mean unit-variance complex random process, λ refers to the signals' wavelength, c symbolizes the propagation speed, and φ_k symbolizes the kth signal's uniformly-distributed random carrier phase.

With a total of N (with $N > K$) snapshots taken at the distinct instances $\{t_n,\ n = 1, \cdots, N\}$, the present direction finding problem is to determine $\{\theta_k, \phi_k,\ k = 1, \cdots, K\}$ from the $6L \times N$ data set: $\boldsymbol{Z} \stackrel{\text{def}}{=} [\boldsymbol{z}(t_1) \ \cdots \ \boldsymbol{z}(t_N)]$ without knowledge of $\boldsymbol{q}(\theta_k, \phi_k)$.[5]

III. Direction-Finding with Arbitrarily Spaced Vector-Sensors at Unknown Locations

A. Overview of Algorithm

The pivotal insight underlying the present algorithm is that the $6L \times 1$ array manifold may be divided into six $(L \times 1)$ subarray manifolds, which are related by invariant factors dependent only on the interrelation among the six electromagnetic-field components of each source's direction-cosines, but not on the vector-sensor's spatial locations. To be precise, the $6L \times 1$ array manifold $\boldsymbol{a}^{(L)}(\theta_k, \phi_k, \gamma_k, \eta_k) = \boldsymbol{a}(\theta_k, \phi_k, \gamma_k, \eta_k) \otimes \boldsymbol{q}(\theta_k, \phi_k)$ may be alternately expressed as

$$\boldsymbol{a}^{(L)}(\theta_k, \phi_k, \gamma_k, \eta_k) = \begin{bmatrix} e_{x_k}\boldsymbol{q}(\theta_k, \phi_k) \\ e_{y_k}\boldsymbol{q}(\theta_k, \phi_k) \\ e_{z_k}\boldsymbol{q}(\theta_k, \phi_k) \\ h_{x_k}\boldsymbol{q}(\theta_k, \phi_k) \\ h_{y_k}\boldsymbol{q}(\theta_k, \phi_k) \\ h_{z_k}\boldsymbol{q}(\theta_k, \phi_k) \end{bmatrix} = \begin{bmatrix} a_1(\theta_k, \phi_k, \gamma_k, \eta_k)\boldsymbol{q}(\theta_k, \phi_k) \\ a_2(\theta_k, \phi_k, \gamma_k, \eta_k)\boldsymbol{q}(\theta_k, \phi_k) \\ a_3(\theta_k, \phi_k, \gamma_k, \eta_k)\boldsymbol{q}(\theta_k, \phi_k) \\ a_4(\theta_k, \phi_k, \gamma_k, \eta_k)\boldsymbol{q}(\theta_k, \phi_k) \\ a_5(\theta_k, \phi_k, \gamma_k, \eta_k)\boldsymbol{q}(\theta_k, \phi_k) \\ a_6(\theta_k, \phi_k, \gamma_k, \eta_k)\boldsymbol{q}(\theta_k, \phi_k) \end{bmatrix} \quad (10)$$

with

$$\boldsymbol{J}_j\boldsymbol{a}^{(L)}(\theta_k, \phi_k) \stackrel{\text{def}}{=} a_j(\theta_k, \phi_k, \gamma_k, \eta_k)\boldsymbol{q}(\theta_k, \phi_k) \quad (11)$$

where $\boldsymbol{J}_j$ is an $L \times 6L$ subarray selection matrix

$$\boldsymbol{J}_j \stackrel{\text{def}}{=} \left[\boldsymbol{O}_{L, L\times(j-1)} \vdots \boldsymbol{I}_L \vdots \boldsymbol{O}_{L, L\times(6-j)}\right], \qquad j = 1, \cdots, 6 \quad (12)$$

and $\boldsymbol{O}_{m,n}$ denotes an $m \times n$ zero matrix and $\boldsymbol{I}_m$ denotes an $m \times m$ identity matrix. Six $L \times K$ subarray manifolds $\{\boldsymbol{A}_j,\ j = 1, \cdots, 6\}$ may thus be formed out of the $6L \times K$ array manifold $\boldsymbol{A}$

$$\boldsymbol{A}_j \stackrel{\text{def}}{=} \boldsymbol{J}_j\boldsymbol{A}, \qquad j = 1, \cdots, 6. \quad (13)$$

These $\{\boldsymbol{A}_1, \cdots, \boldsymbol{A}_6\}$ subarray manifolds are interrelated as follows:

$$\boldsymbol{A}_{j+1} = \boldsymbol{A}_j \underbrace{\begin{bmatrix} \chi_1^{(j,j+1)} & & \\ & \ddots & \\ & & \chi_K^{(j,j+1)} \end{bmatrix}}_{\stackrel{\text{def}}{=} \boldsymbol{X}^{(j,j+1)}} \quad (14)$$

where $\chi_k^{(j,j+1)} \stackrel{\text{def}}{=} (a_{j+1}(\theta_k, \phi_k, \gamma_k, \eta_k)/a_j(\theta_k, \phi_k, \gamma_k, \eta_k))$. In other words, the matrix pencil $\{\boldsymbol{A}_j, \boldsymbol{A}_{j+1}\}$ has generalized

[4]These incident signals are narrow-band in that their bandwidths are very small compared to the inverse of the wavefronts' transit time across the array. The case involving broad-band signals may be reduced to a set of narrow-band problems via a comb of narrow-band filters.

[5]Although the proposed algorithm will be presented in the batch processing mode; however, real-time adaptive implementations of this present algorithm may be readily realized for nonstationary environments using the fast recursive eigendecomposition updating methods such as that in [15].

eigenvalues equal to $\{\chi_k^{(j,j+1)},\ k = 1, \cdots, K\}$. Note that none of $\{\chi^{(j,j+1)},\ k = 1, \cdots, K,\ j = 1, \cdots, 5\}$ depends on the vector-sensors' locations $\{(x_l, y_l, z_l),\ l = 1, \cdots, L\}$. The foregoing analysis thus suggests that without any constraint on nor any knowledge of the location of any of the vector-sensors, application of ESPRIT to the matrix-pencil in (14) would estimate the invariant factors $\{\chi_k^{(j,j+1)},\ j = 1, \cdots, 5\}$[6] among the kth source's six electromagnetic-field components $\{\boldsymbol{a}_j(\theta_k, \phi_k, \gamma_k, \eta_k),\ j = 1, \cdots, 6\}$. Note that ESPRIT may be applied to the five matrix pencils $\{(\boldsymbol{A}_j, \boldsymbol{A}_{j+1}),\ j = 1, \cdots, 5\}$ in parallel to facilitate real-time implementation.

B. Subspace Decomposition

In eigenstructure (subspace) direction finding methods such as ESPRIT, the overall data correlation matrix $\boldsymbol{Z}\boldsymbol{Z}^H$ [which embodies a maximum likelihood (ML) estimate of the true sample correlation matrix if the additive noise is Gaussian] is decomposed into a K-dimensional signal subspace and a $(6L-K)$-dimensional noise subspace. Therefore, the first step in the proposed algorithm is to compute the K $(6L \times 1)$ signal-subspace eigenvectors by eigen-decomposing the $6L \times 6L$ data correlation matrix $\boldsymbol{R}_{zz} = \boldsymbol{Z}\boldsymbol{Z}^H$. Let $\boldsymbol{E}_s$ be the $6L \times K$ matrix composed of the K eigenvectors corresponding to the K largest eigenvalues of $\boldsymbol{R}_{zz}$; and let let $\boldsymbol{E}_n$ denote the $6L \times (6L-K)$ matrix composed of the remaining $6L - K$ eigenvectors of $\boldsymbol{Z}\boldsymbol{Z}^H$:

$$\boldsymbol{R}_{zz} = \boldsymbol{Z}\boldsymbol{Z}^H = \frac{1}{N}\sum_{i=1}^{N} \boldsymbol{z}(t_i)\boldsymbol{z}^H(t_i) = \boldsymbol{E}_s\boldsymbol{D}_s\boldsymbol{E}_s^H + \boldsymbol{E}_n\boldsymbol{D}_n\boldsymbol{E}_n^H \tag{15}$$

where

$$\boldsymbol{E}_s \approx \boldsymbol{A}\boldsymbol{T} = [\boldsymbol{a}(\theta_1, \phi_1, \gamma_1, \eta_1) \otimes \boldsymbol{q}(\theta_1, \phi_1), \cdots, \boldsymbol{a}(\theta_K, \phi_K, \gamma_K, \eta_K) \otimes \boldsymbol{q}(\theta_K, \phi_K)]\boldsymbol{T} \tag{16}$$

and $\boldsymbol{T}$ represents an unknown but nonsingular $K \times K$ coupling matrix $\boldsymbol{D}_s$ denotes a $K \times K$ diagonal matrix whose diagonal entries are the K largest eigenvalues, and $\boldsymbol{D}_n$ symbolizes a $(6L-K) \times (6L-K)$ diagonal matrix whose diagonal entries contains the $6L-K$ smallest eigenvalues. $\boldsymbol{T}$ is nonsingular because both $\boldsymbol{E}_s$ and $\boldsymbol{A}$ are full rank. If there existed no noise or if an infinite number of snapshots were available; the approximation would become exact.

C. Estimation of $\{\chi_k^{(j,j+1)},\ k = 1, \cdots, K\}$

Analogous to (14), $\boldsymbol{J}_j$ and $\boldsymbol{J}_{j+1}$ are next used to construct the signal-subspace matrix pencil $\{\boldsymbol{E}_{s,j}, \boldsymbol{E}_{s,j+1}\}$

$$\boldsymbol{E}_{s,j} = \boldsymbol{J}_j\boldsymbol{E}_s \approx \boldsymbol{A}_j\boldsymbol{T} \tag{17}$$

$$\boldsymbol{E}_{s,j+1} = \boldsymbol{J}_{j+1}\boldsymbol{E}_s \approx \boldsymbol{A}_{j+1}\boldsymbol{T}. \tag{18}$$

[6]After the camera-ready copy of this manuscript has been submitted, the first author recognized that the $\{\boldsymbol{A}_3, \boldsymbol{A}_4\}$ matrix pencil need not be processed, as will be explained in a footnote in Section III-D.

There exists a $K \times K$ nonsingular matrix $\boldsymbol{\Psi}^{(j,j+1)}$ relating the two $L \times K$ full-ranked matrices $\boldsymbol{E}_{s,j}$ and $\boldsymbol{E}_{s,j+1}$ [1]

$$\boldsymbol{E}_{s,j}\boldsymbol{\Psi}^{(j,j+1)} = \boldsymbol{E}_{s,j+1} \Rightarrow \boldsymbol{\Psi}^{(j,j+1)} = \left((\boldsymbol{E}_{s,j})^H\boldsymbol{E}_{s,j}\right)^{-1}\left((\boldsymbol{E}_{s,j})^H\boldsymbol{E}_{s,j+1}\right) \tag{19}$$

$$\Rightarrow \boldsymbol{\Psi}^{(j,j+1)} \approx \left(\boldsymbol{T}^{(j,j+1)}\right)^{-1}\hat{\boldsymbol{X}}^{(j,j+1)}\boldsymbol{T}^{(j,j+1)} \tag{20}$$

where

$$\boldsymbol{T}^{(j,j+1)} = \boldsymbol{P}^{(j,j+1)}\boldsymbol{T} \tag{21}$$

and $\boldsymbol{P}^{(j,j+1)}$ represents some unknown permutation matrix whose kth column equals a $K \times 1$ vector with all zeroes except a one at the i_kth position and $\{i_1, \cdots, i_K\}$ is some permutation of $\{1, \cdots, K\}$. Equation (20) is obtained from equation (19) by substituting equations (14), (17) and (18) into equation (19). This unknown permutation of the rows of $\boldsymbol{T}$ [i.e., the permutation of the eigenvectors of $\boldsymbol{\Psi}^{(j,j+1)}$] as columns of $(\boldsymbol{T}^{(j,j+1)})^{-1}$ arises in the eigendecomposition of $\boldsymbol{\Psi}^{(j,j+1)}$—(20) still holds replacing $\boldsymbol{T}$ and $\boldsymbol{X}^{(j,j+1)}$, respectively, by $\boldsymbol{P}^{(j,j+1)}\boldsymbol{T}$ and $\boldsymbol{P}^u\boldsymbol{X}^{(j,j+1)}(\boldsymbol{P}^u)^{-1}$. From these, the invariant factor $\chi_k^{(j,j+1)}$ between the $a_{j+1}(\theta_k, \phi_k, \gamma_k, \eta_k)$ and $a_j(\theta_k, \phi_k, \gamma_k, \eta_k)$ may be estimated for each of the K sources

$$\hat{\chi}_{k^{(j)}}^{(j,j+1)} \approx \left[\boldsymbol{X}^{(j,j+1)}\right]_{kk}, \qquad k = 1, \cdots, K \tag{22}$$

where $\{[\boldsymbol{X}^{(j,j+1)}]_{kk},\ k = 1, \cdots, K\}$ constitute the diagonal elements of the diagonal matrix $\boldsymbol{X}^{(j,j+1)}$ and are approximated by the eigenvalues of $\boldsymbol{\Psi}^{(j,j+1)}$. [The reason for the superscript (j) in k will become clear shortly.] Furthermore, the eigenvector corresponding to the eigenvalue $[\boldsymbol{X}^{(j,j+1)}]_{kk}$ constitutes the kth column of $(\boldsymbol{T}^{(j,j+1)})^{-1}$.

Note that different indexes are used to enumerate $\hat{\chi}_k^{(j,j+1)}$ for different values of j and that in general $\boldsymbol{T}^{(j,j+1)} \neq \boldsymbol{T}^{(i,i+1)}$ for $j \neq i$, even though $\boldsymbol{\Psi}^{(j,j+1)}$ and $\boldsymbol{\Psi}^{(i,i+1)}$ share the same set of eigenvectors. That is, the eigenvectors are ordered differently in $(\boldsymbol{T}^{(j,j+1)})^{-1}$ as in $(\boldsymbol{T}^{(i,i+1)})^{-1}$. No mismatch, however, exists between $\hat{\chi}_k^{(j,j+1)}$ and its corresponding eigenvector, namely the kth column of $(\boldsymbol{T}^{(j,j+1)})^{-1}$. This is true for all $j \in \{1, \cdots, 5\}$. Thus, $\hat{\chi}_{k^{(j)}}^{(j,j+1)}$ may be paired with $\hat{\chi}_{k^{(i)}}^{(i,i+1)}$ from the same source by matching the orthogonal rows of $\boldsymbol{T}^{(j,j+1)}$ with those of $\boldsymbol{T}^{(i,i+1)}$ as follows. Let $(k^{(j)}, k^{(i)})$ denote the row index of the matrix element with the largest absolute value in the $k^{(i)}$th column of the $K \times K$ matrix $\boldsymbol{T}^{(i,i+1)}(\boldsymbol{T}^{(j,j+1)})^{-1}$. Then $\hat{\chi}_{k^{(j)}}$ and $\hat{\chi}_{k^{(i)}}$ belong to the same source. Note that this pairing procedure involves minimum computation and requires *no* exhaustive searches. An alternate pairing method requiring more computation but offering possibly more robust pairing is available in [7].

D. DOA Estimation via Vector-Sensor Product

The algorithm thus far is entirely parallel to that in [8]. With up to $\binom{6}{2\,2\,2}/3! = 15$ distinct pairings among the six electromagnetic field components, there are available up to 15 nonlinear equations relating the four unknown signal parameters

$\{\theta_k, \phi_k, \gamma_k, \eta_k\}$. Li [8] then derived closed-form expressions for these four parameters based on clever but complicated manipulation of these 15 nonlinear equations. Instead, the present algorithm will suggest a simpler and more elegant approach based on the recognition that: 1) preceding algorithmic steps have already estimated the six-component electromagnetic field vector to within a complex constant and 2) this result will be sufficient to determine uniquely the corresponding normalized Poynting vector.

Because $\chi_k^{(j,j+1)}$ embodies the ratio between $a_{j+1}(\theta_k, \phi_k, \gamma_k, \eta_k)$ and $a_j(\theta_k, \phi_k, \gamma_k, \eta_k)$ under noiseless conditions

$$\hat{\boldsymbol{a}}(\theta_k, \phi_k, \gamma_k, \eta_k) = r_k e^{j\alpha_k} \begin{bmatrix} 1 \\ \chi_k^{(1,2)} \\ \chi_k^{(1,2)}\chi_k^{(2,3)} \\ \chi_k^{(1,2)}\chi_k^{(2,3)}\chi_k^{(3,4)} \\ \chi_k^{(1,2)}\chi_k^{(2,3)}\chi_k^{(3,4)}\chi_k^{(4,5)} \\ \chi_k^{(1,2)}\chi_k^{(2,3)}\chi_k^{(3,4)}\chi_k^{(4,5)}\chi_k^{(5,6)} \end{bmatrix} \tag{23}$$

where r_k represents a real scalar, $0 \le \alpha_k < 2\pi$, and $r_k e^{j\alpha_k} = e_{x_k}$. Thus, under noisy conditions

$$\hat{\boldsymbol{p}}_k = \hat{e}_k \times \hat{h}_k^* = \begin{bmatrix} \hat{u}_k \\ \hat{v}_k \\ \hat{w}_k \end{bmatrix} \tag{24}$$

$$= \left(r_k e^{j\alpha_k} \begin{bmatrix} 1 \\ \chi_k^{(1,2)} \\ \chi_k^{(1,2)}\chi_k^{(2,3)} \end{bmatrix} \right) \times \left(r_k e^{j\alpha_k} \begin{bmatrix} \chi_k^{(1,2)}\chi_k^{(2,3)}\chi_k^{(3,4)} \\ \chi_k^{(1,2)}\chi_k^{(2,3)}\chi_k^{(3,4)}\chi_k^{(4,5)} \\ \chi_k^{(1,2)}\chi_k^{(2,3)}\chi_k^{(3,4)}\chi_k^{(4,5)}\chi_k^{(5,6)} \end{bmatrix} \right)^* \tag{25}$$

$$= (\|r_k\|^2) \left(\begin{bmatrix} 1 \\ \chi_k^{(1,2)} \\ \chi_k^{(1,2)}\chi_k^{(2,3)} \end{bmatrix} \times \begin{bmatrix} \chi_k^{(1,2)}\chi_k^{(2,3)}\chi_k^{(3,4)} \\ \chi_k^{(1,2)}\chi_k^{(2,3)}\chi_k^{(3,4)}\chi_k^{(4,5)} \\ \chi_k^{(1,2)}\chi_k^{(2,3)}\chi_k^{(3,4)}\chi_k^{(4,5)}\chi_k^{(5,6)} \end{bmatrix}^* \right). \tag{26}$$

However, because $\mathcal{P}_k = 1$, (27), shown at the bottom of the page, holds. Hence, the kth impinging source's Cartesian direction-cosine estimates are as shown in (28), at the bottom of the page.[7] Thus, the complex scalar ambiguity of $r_k e^{j\alpha_k}$ in (23) causes no ambiguity in the direction cosine estimates. Note that it is unnecessary to know or to compute the inter-vector-sensor spatial phase delays to resolve the incident signals, so long as the array spacing has an unambiguous geometry (with respect to the azimuth angle and the elevation angle), which is generally the case for a randomly placed array of sensors. However, if the array grid geometry is ambiguous, then the number of resolvable sources may drop below L and equals the number of resolvable sources by one vector-sensor—an issue investigated by [16].

[7]After the camera-ready copy of this manuscript has been submitted, the first author realized that

$$\begin{bmatrix} \chi_k^{(1,2)}\chi_k^{(2,3)}\chi_k^{(3,4)} \\ \chi_k^{(1,2)}\chi_k^{(2,3)}\chi_k^{(3,4)}\chi_k^{(4,5)} \\ \chi_k^{(1,2)}\chi_k^{(2,3)}\chi_k^{(3,4)}\chi_k^{(4,5)}\chi_k^{(5,6)} \end{bmatrix}$$

may be substituted by

$$\begin{bmatrix} 1 \\ \chi_k^{(4,5)} \\ \chi_k^{(4,5)}\chi_k^{(5,6)} \end{bmatrix}.$$

This means that $\{\chi_k^{(3,4)},\ \ k = 1, \cdots, K\}$ need not be evaluated.

$$r_k^2 = \frac{1}{\left(\left\| \begin{bmatrix} 1 \\ \chi_k^{(1,2)} \\ \chi_k^{(1,2)}\chi_k^{(2,3)} \end{bmatrix} \right\| \right) \left(\left\| \begin{bmatrix} \chi_k^{(1,2)}\chi_k^{(2,3)}\chi_k^{(3,4)} \\ \chi_k^{(1,2)}\chi_k^{(2,3)}\chi_k^{(3,4)}\chi_k^{(4,5)} \\ \chi_k^{(1,2)}\chi_k^{(2,3)}\chi_k^{(3,4)}\chi_k^{(4,5)}\chi_k^{(5,6)} \end{bmatrix} \right\| \right)} \tag{27}$$

$$\begin{bmatrix} \hat{u}_k \\ \hat{v}_k \\ \hat{w}_k \end{bmatrix} = \frac{\begin{bmatrix} 1 \\ \chi_k^{(1,2)} \\ \chi_k^{(1,2)}\chi_k^{(2,3)} \end{bmatrix} \times \begin{bmatrix} \chi_k^{(1,2)}\chi_k^{(2,3)}\chi_k^{(3,4)} \\ \chi_k^{(1,2)}\chi_k^{(2,3)}\chi_k^{(3,4)}\chi_k^{(4,5)} \\ \chi_k^{(1,2)}\chi_k^{(2,3)}\chi_k^{(3,4)}\chi_k^{(4,5)}\chi_k^{(5,6)} \end{bmatrix}^*}{\left(\left\| \begin{bmatrix} 1 \\ \chi_k^{(1,2)} \\ \chi_k^{(1,2)}\chi_k^{(2,3)} \end{bmatrix} \right\| \right) \left(\left\| \begin{bmatrix} \chi_k^{(1,2)}\chi_k^{(2,3)}\chi_k^{(3,4)} \\ \chi_k^{(1,2)}\chi_k^{(2,3)}\chi_k^{(3,4)}\chi_k^{(4,5)} \\ \chi_k^{(1,2)}\chi_k^{(2,3)}\chi_k^{(3,4)}\chi_k^{(4,5)}\chi_k^{(5,6)} \end{bmatrix} \right\| \right)} \tag{28}$$

E. Azimuth Angle, Elevation Angle, and Polarization Parameter Estimates

From the direction-cosine estimates derived above, the kth signal's azimuth and elevation arrival angles may be estimated as

$$\hat{\theta}_k = \sin^{-1}\sqrt{\hat{u}_k^2 + \hat{v}_k^2} = \cos^{-1}\hat{w}_k \tag{29}$$

$$\hat{\phi}_k = \tan^{-1}|\hat{v}_k/\hat{u}_k|. \tag{30}$$

Note that once the $\{\chi_k^{(j,j+1)},\ j = 1, \cdots, 5;\ k = 1, \cdots, K\}$ are paired, the azimuth and elevation estimates are also automatically matched with no additional processing. The polarization parameters of the kth signal may then be estimated as

$$\hat{\gamma}_k = \tan^{-1}|\hat{g}_{k_1}/\hat{g}_{k_2}|$$
$$\hat{\eta}_k = \angle\hat{g}_{k_1} - \angle\hat{g}_{k_2}$$

where

$$\hat{\boldsymbol{g}}_k = \begin{bmatrix}\hat{g}_{k_1}\\ \hat{g}_{k_2}\end{bmatrix} = \left[\boldsymbol{\Theta}_k^H(\hat{\theta}_k, \hat{\phi}_k)\boldsymbol{\Theta}_k(\hat{\theta}_k, \hat{\phi}_k)\right]^{-1}\boldsymbol{\Theta}_k^H(\hat{\theta}_k, \hat{\phi}_k)\hat{\boldsymbol{a}}_k.$$

IV. Calibration and Remedy for Vector-Sensor Misorientation

This algorithm requires no geometric regularity in and no *a priori* knowledge of the inter-vector-sensor spacings; however, the foregoing development (and that by Li [8]) presumes all vector-sensors to be identically aligned. This section will analyze the effects of nonidentical orientation or random orientation. A basic calibration method and a simple remedy will also be presented to illustrate the possibility of modifying the foregoing algorithm to accommodate electromagnetic vector-sensor misorientation. Note that effects of and remedies for such misorientation were not discussed in [8].

Effects of Vector-Sensor Misorientation: Suppose that the lth vector-sensor deviates from its nominal orientation such that the antennas nominally aligned along the x-axis is actually aligned along the $\tilde{x}_l$-axis and, similarly, for the y-axis and the z-axis. This $(\tilde{x}_l, \tilde{y}_l, \tilde{z}_l)$ coordinate system may be constructed from the (x, y, z) coordinate system by: 1) a $\tilde{\phi}_l$ rotation about the z-axis and then 2) a $\tilde{\theta}_l$ rotation about the newly constructed $\tilde{x}_l$-axis. [Note that the order of these two steps are not commutable, because $\{\tilde{\theta}_l, \tilde{\phi}_l\}$ does not uniquely relates $(\tilde{x}_l, \tilde{y}_l, \tilde{z}_l)$ to (x, y, z).] Thus, any signal incident from the direction $\{u(\theta_k, \phi_k), v(\theta_k, \phi_k), w(\theta_k)\}$ would become misidentified as coming from $\{\tilde{u}(\theta_k^{(l)}, \phi_k^{(l)}), \tilde{v}(\theta_k^{(l)}, \phi_k^{(l)}), \tilde{w}(\theta_k^{(l)})\}$, where

$$\begin{bmatrix}\tilde{u}\left(\theta_k^{(l)}, \phi_k^{(l)}\right)\\ \tilde{v}\left(\theta_k^{(l)}, \phi_k^{(l)}\right)\\ \tilde{w}\left(\theta_k^{(l)}\right)\end{bmatrix} = \underbrace{\begin{bmatrix}1 & 0 & 0\\ 0 & \cos\tilde{\theta}_l & \sin\tilde{\theta}_l\\ 0 & -\sin\tilde{\theta}_l & \cos\tilde{\theta}_l\end{bmatrix}\begin{bmatrix}\cos\tilde{\phi}_l & -\sin\tilde{\phi}_l & 0\\ \sin\tilde{\phi}_l & \cos\tilde{\phi}_l & 0\\ 0 & 0 & 1\end{bmatrix}}_{\stackrel{\text{def}}{=}\tilde{\boldsymbol{R}}_l} \times \begin{bmatrix}u(\theta_k, \phi_k)\\ v(\theta_k, \phi_k)\\ w(\theta_k)\end{bmatrix}. \tag{31}$$

Calibration of Vector-Sensor Misorientation: Calibration algorithms of various degrees of sophistication and capability may be devised to determine the state of misorientation of each vector-sensor in the array. A rather simplistic calibration algorithm will be introduced below using three reference signals. This rather unsophisticated method is used only as an illustration. More sophisticated alternatives, perhaps with self-calibration capabilities, are currently under development.

Suppose three reference signals from known directions-of-arrival, $\{(\theta_1, \phi_1), (\theta_2, \phi_2), (\theta_3, \phi_3)\}$, incident upon the array in use. Further, suppose that the spectra of all three reference signals are nonoverlapping among themselves nor with the spectra of any other signals. Then each of the three reference signals may be easily isolated from the sampled data by passing the sampled data through a bandpass filter with the appropriate passband.

The misoriented normalized Poynting vector $\tilde{\boldsymbol{p}}^{(l)}(\theta_k, \phi_k)$ is related to the nominal direction-cosines $\{u(\theta_k, \phi_k), v(\theta_k, \phi_k), w(\theta_k)\}$ as

$$\tilde{\boldsymbol{p}}^{(l)}(\theta_k, \phi_k) \stackrel{\text{def}}{=} \begin{bmatrix}u(\tilde{\theta}_k, \tilde{\phi}_k)\\ v(\tilde{\theta}_k, \tilde{\phi}_k)\\ w(\tilde{\theta}_k)\end{bmatrix} = \tilde{\boldsymbol{R}}_l\begin{bmatrix}u(\theta_k, \phi_k)\\ v(\theta_k, \phi_k)\\ w(\theta_k)\end{bmatrix}. \tag{32}$$

The 3×3 coordinate rotational matrix $\tilde{\boldsymbol{R}}_l$ may be determined with the three reference signals because $\{u(\theta_k, \phi_k), v(\theta_k, \phi_k), w(\theta_k)\}$ are known *a priori* and $\{\tilde{\boldsymbol{p}}^{(l)}(\theta_k, \phi_k),\ k = 1, 2, 3\}$ may be measured as discussed above. Thus

$$\tilde{\boldsymbol{R}} = \tilde{\boldsymbol{A}}_l^r(\boldsymbol{A}^r)^{-1} \tag{33}$$

where

$$\boldsymbol{A}^r \stackrel{\text{def}}{=} \begin{bmatrix}u(\theta_1, \phi_1) & u(\theta_2, \phi_2) & u(\theta_3, \phi_3)\\ v(\theta_1, \phi_1) & v(\theta_2, \phi_2) & v(\theta_3, \phi_3)\\ w(\theta_1) & w(\theta_2) & w(\theta_3)\end{bmatrix} \tag{34}$$

$$\tilde{\boldsymbol{A}}_l^r \stackrel{\text{def}}{=} \left[\tilde{\boldsymbol{p}}^{(l)}(\theta_1, \phi_1)\quad \tilde{\boldsymbol{p}}^{(l)}(\theta_2, \phi_2)\quad \tilde{\boldsymbol{p}}^{(l)}(\theta_3, \phi_3)\right]. \tag{35}$$

Remedy for Vector-Sensor Misorientation: Having identified the true orientation of each vector-sensor by the foregoing calibration algorithm, the original direction finding algorithm may be modified as follows to accommodate each vector-sensor's misorientation:

$$\tilde{\boldsymbol{Z}} \stackrel{\text{def}}{=} \tilde{\boldsymbol{R}}\boldsymbol{Z} \tag{36}$$

where

$$\tilde{\boldsymbol{R}} \stackrel{\text{def}}{=} \begin{bmatrix}\tilde{\boldsymbol{R}}_1 & & \\ & \ddots & \\ & & \tilde{\boldsymbol{R}}_L\end{bmatrix}. \tag{37}$$

The original direction finding algorithm can now be applied with $\tilde{\boldsymbol{Z}}$ substituting for $\boldsymbol{Z}$. Note that under noisy and

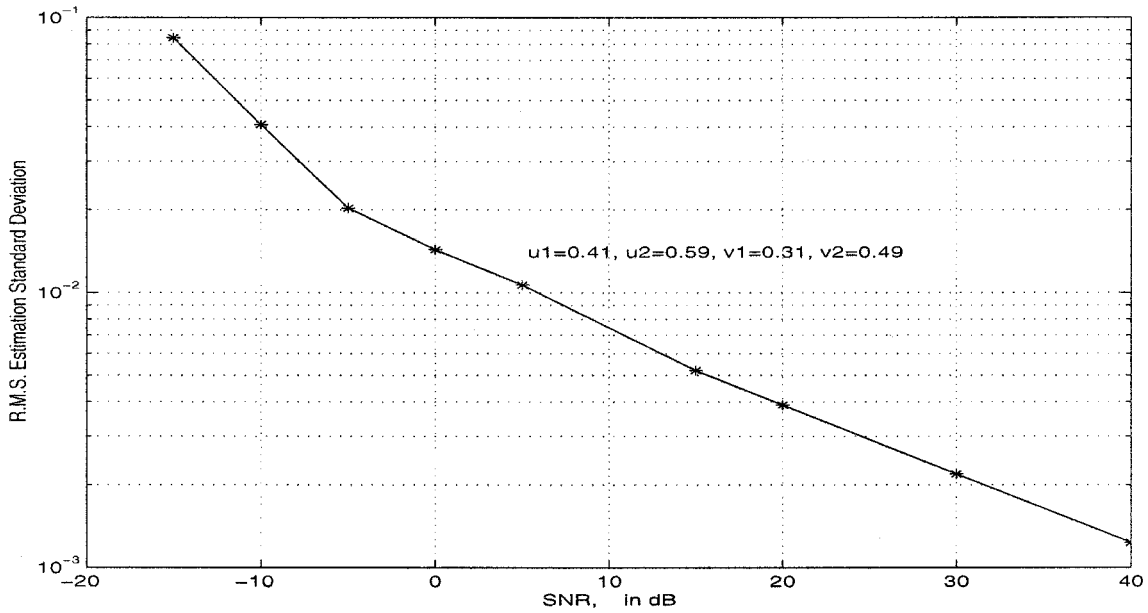

Fig. 1. RMS standard deviation of $\{\hat{u}_1, \hat{u}_2, \hat{v}_1, \hat{v}_2\}$ versus SNR: two closely spaced equal-power uncorrelated narrow-band sources with $\theta_1 = 58.07°$, $\phi_1 = 44.05°$, $\mathcal{P}_1 = 1$, $\theta_2 = 59.10°$, $\phi_2 = 36.47°$, $\mathcal{P}_2 = 1$, $\gamma_1 = \gamma_2 = \pi/4$, $\eta_1 = -\eta_2 = \pi/2$ impinge upon a 13-element nonuniformly spaced 3-D array, 200 snapshots per experiment, 500 independent experiments per data point. The vector-sensors may be: 1) randomly oriented and direction-cosines estimates are obtained using the orientational calibration/correction procedure and/or 2) perfectly paired using *a priori* source information.

nonasymptotic situations, $\tilde{\boldsymbol{R}}$ would be estimated with nonzero error, thereby adding another error source toward the estimation error in $\{\hat{\phi}_k, \hat{\theta}_k, \quad k = 1, \cdots, K\}$. This is admittedly a rather crude remedy; more sophisticated remedies are under development.

V. Simulations

Simulation results presented in Figs. 1–5 verify the efficacy of the proposed closed-form direction finding and polarization estimation algorithm for arbitrarily spaced electromagnetic vector-sensors at unknown locations. For all figures, two closely spaced equal-power uncorrelated narrow-band sources impinge upon a 13-element irregularly spaced 3-D array of vector-sensors. This array may be considered as a nine-element nonuniformly spaced cross-shaped array with elements at the Cartesian coordinates $(\lambda/2) \times \{(0, 0, 0), (\pm 1, 0, 0)(\pm 2.7, 0, 0), (0, \pm 1, 0), (0, \pm 2.7, 0)\}$ plus a four-element square array with elements at the Cartesian coordinates $(\lambda/2) \times \{(\pm 4, \pm 4, 1)\}$. The two closely spaced equal-power uncorrelated narrow-band sources have the following parameter values: $\theta_1 = 30.93°$, $\phi_1 = 37.09°$, $\theta_2 = 50.08°$, $\phi_2 = 39.71°$. (That is, the first source has $u_1 = 0.41$ and $v_1 = 0.31$, and the second source has $u_2 = 0.59$ and $v_2 = 0.49$.) The polarization states are $\gamma_1 = 45°$, $\eta_1 = 90°$, $\gamma_2 = 45°$, $\eta_2 = -90°$. The additive white noise is complex Gaussian; and the SNR is defined relative to each source. Two-hundred snapshots are used in each of the 500 independent Monte Carlo simulation experiments.

The solid curves with circular data points in Figs. 1and 2, respectively, plot the direction-cosines' composite estimation standard deviation and bias, respectively, at various signal-to-noise ratio (SNR) levels, using the proposed pairing procedure. The composite RMS standard deviation plotted is computed by taking the square root of the mean of the respective variances of $\hat{u}$ and $\hat{v}$; and the composite bias is similarly computed by taking the square root of the mean of the square of the respective sample biases of $\hat{u}$ and $\hat{v}$. Note that $u_2 - u_1 = v_1 - v_2 = 0.18$; thus, the two sources would be resolved and identified with high probability if both the estimation standard deviation and the bias are under approximately 0.05. The proposed ESPRIT-based algorithm successfully resolves these closely-spaced sources for all SNR's at or above -10 dB. Above these SNR resolution thresholds, estimation standard deviation and bias both decrease fairly linearly with increasing SNR decibel values.

Figs. 3 and 4, respectively, plot the polarization parameters' composite estimation standard deviation and bias at different SNR levels. The RMS values are defined similarly as in Figs. 1 and 2. In the SNR range (namely, at or above -10 dB) where the Cartesian direction cosines are successfully resolved, the polarization parameters are estimated to within 0.002π in bias and 0.03π in standard deviation. For SNR's above 0 dB, estimation standard deviation and bias both decrease fairly linearly with increasing SNR dB values.

Figs. 1, 2, and 5 verify the effectiveness of the proposed calibration and correction procedure for the case where the vector-sensors' orientations are unknown and need to be calibrated. The "*" data points refer to an array of vector-sensors with unknown random orientation, with each parameter in $\{(\tilde{\theta}_l, \tilde{\phi}_l), \quad l = 1, \cdots, L\}$ independently and uniformly distributed over $[0, \pi/2)$ and independently generated in each simulation run. The "o" data points refer to an array of vector-sensors with identical and known orientation. The solid curve uses the proposed procedure to calibrate and correct the misorientation. The dashed curve forced perfect pairing using information regarding the sources' true

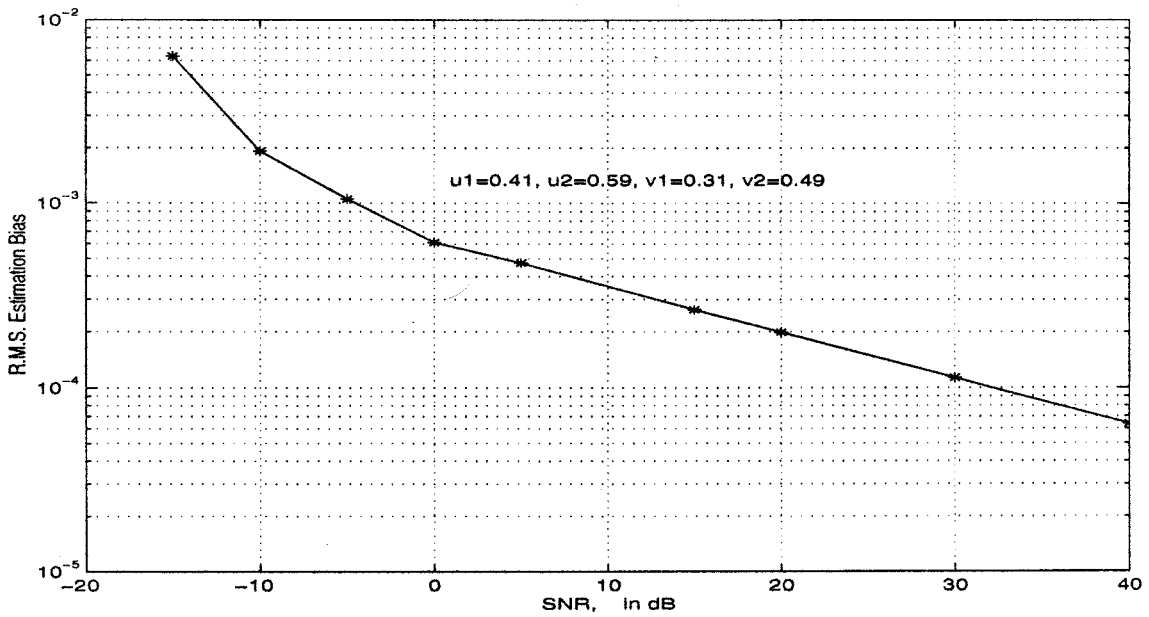

Fig. 2. RMS bias of $\{\hat{u}_1, \hat{u}_2, \hat{v}_1, \hat{v}_2\}$ versus SNR: same settings as in Fig. 1.

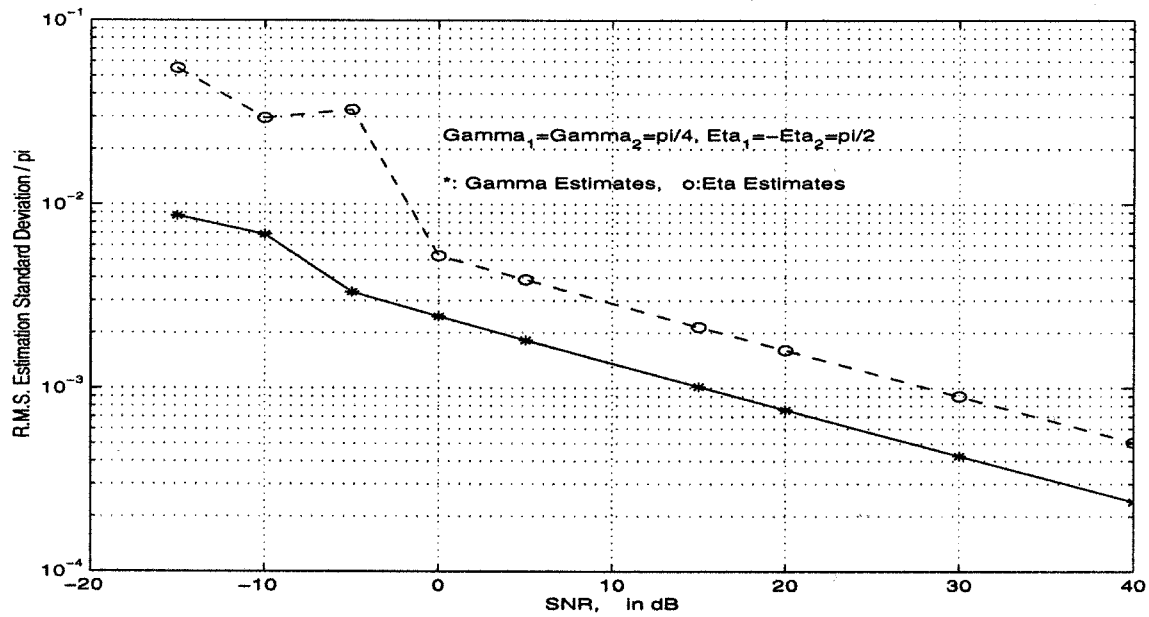

Fig. 3. RMS standard deviation of $\{\hat{\gamma}_1, \hat{\gamma}_2, \hat{\eta}_1, \hat{\eta}_2\}$ versus SNR: same settings as in Fig. 1, but all vector-sensors are identically oriented and the direction-cosine estimates are paired as proposed.

incident angles. Three calibration sources, at the same frequency as the unknown incident sources but with the angular and polarization parameters $u_1 = 0.2,\ u_2 = 0.5,\ u_3 = 0.7$; $v_1 = 0.8,\ v_2 = 0.3,\ v_3 = 0.6$; $\gamma_1 = \gamma_2 = \pi/4,\ \gamma_3 = 0$; $\eta_1 = -\eta_2 = \pi/2,\ \eta_3 = 0$ are sampled 200 times at the sampling frequency as for the incident sources. From Fig. 5, there exists no mispairing among all 500 independent simulation runs for all SNR above 0 dB. Comparing the two curves in Figs. 1 and 2 with "o" data points, the proposed pairing procedure works well—nowhere does mispairing costs more than 2 dB in SNR relative to the perfectly paired case. Comparing the two curves in Figs. 1 and 2 with "*" data points for the randomly oriented array, nowhere in the SNR range tested does the proposed pairing procedure costs more than 2–3 dB in SNR, when used with the proposed calibration and correction procedure. Based on the closeness of the two "*" curves in Fig. 1, the relatively poor performance at low SNR (with estimation standard deviation of 0.5 at -20 dB) for

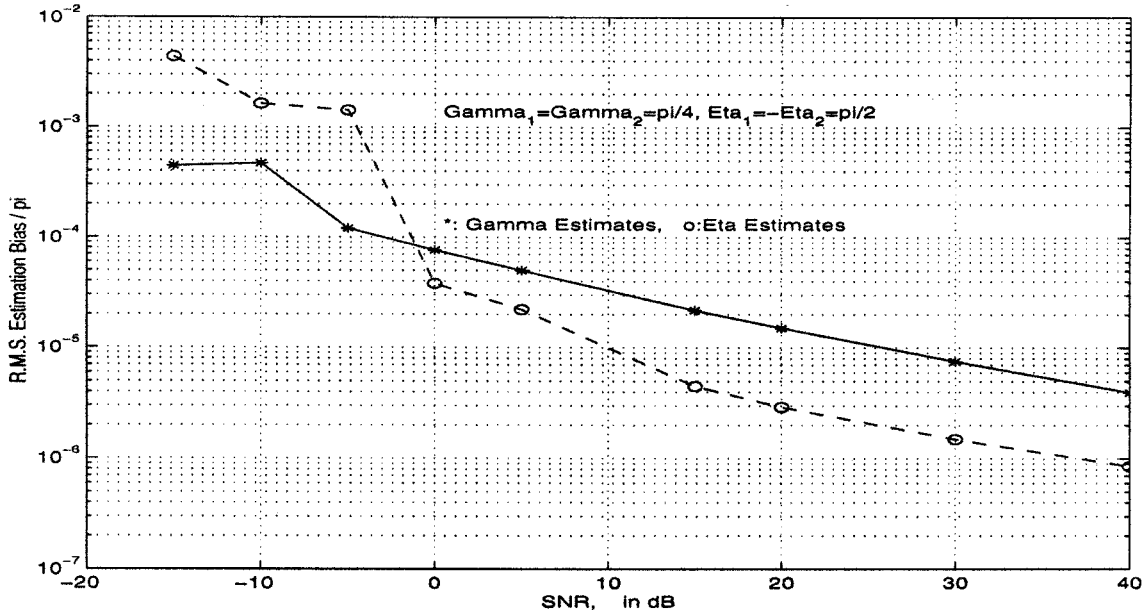

Fig. 4. RMS bias of $\{\hat{\gamma}_1, \hat{\gamma}_2, \hat{\eta}_1, \hat{\eta}_2\}$ versus SNR: same settings as in Fig. 3.

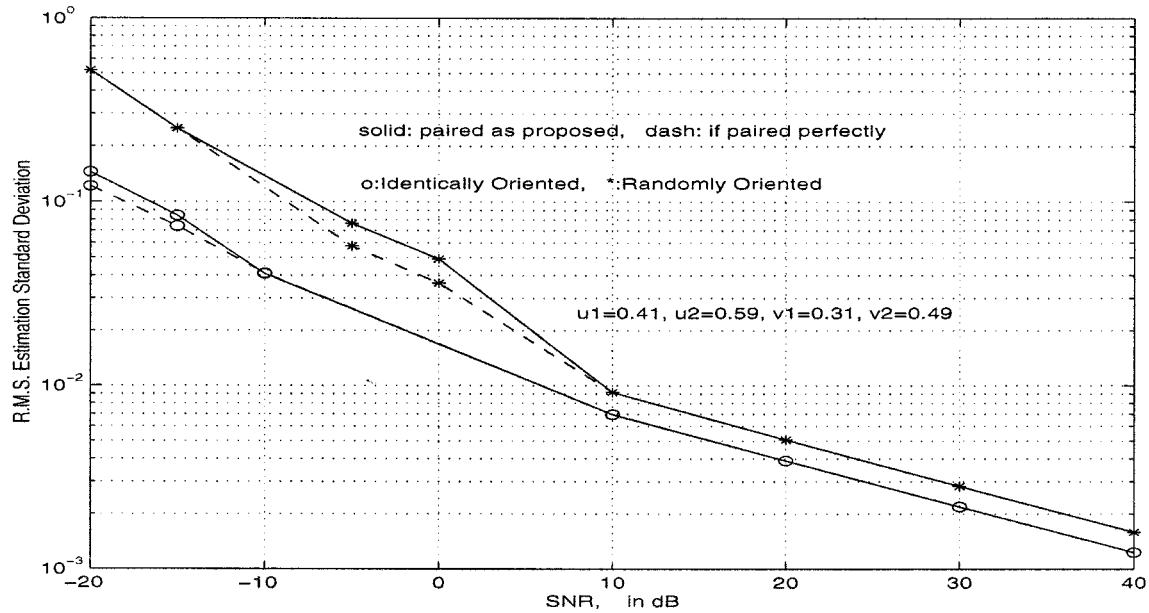

Fig. 5. Percentage of runs where the Cartesian direction cosines are mispaired versus SNR: same settings as in Fig. 3.

the randomly oriented array is NOT due to mispairing errors but due to general breakdown in array resolution. However, comparing the "*" curves with the "o" curves, random orientation does cost 4–10 dB in SNR in the present signal scenario. While the identically oriented array produces more biased estimates for all SNR above 13 dB, the estimation bias is generally at least an order of magnitude less than the corresponding estimation standard deviation and thus does not substantially affect the above analysis.

VI. Conclusion

The proposed ESPRIT-based electromagnetic direction finding and polarization estimation algorithm offers closed-form solutions to arbitrarily spaced arrays of electromagnetic vector-sensors whose locations need not be known. The vector-sensors' spatial location may remain unknown because ESPRIT's invariance factors no longer depend on array geometry. This advantage alleviates the nontrivial problem of

spatial calibration, though the vector-sensors still need to be identically oriented. A basic calibration and remedy have also been verified as efficacious to accommodate vector-sensor misorientation. This algorithm is readily susceptible to parallel implementation, thereby facilitating real-time uses. Using the technique in [28], the present scheme also works by substituting each six-component vector-sensor by a dipole triad or by a loop triad. Though the proposed algorithm is presented in the batch processing mode, real-time adaptive implementations of this present algorithm may be readily realized for nonstationary environments using the fast recursive eigendecomposition updating methods such as that in [15].

REFERENCES

[1] R. O. Schmidt, "Multiple emitter location and signal parameter estimation," in *RADC Spectral Estimation Workshop*, 1979.

[2] M. Kanda, "An electromagnetic near-field sensor for simultaneous electric and magnetic-field measurements," *IEEE Trans. Electromagn. Compat.*, vol. EMC-26, pp. 102–110, Aug. 1984.

[3] R. Roy and T. Kailath, "ESPRIT-estimation of signal parameters via rotational invariance techniques," *IEEE Trans. Acoust., Speech, Signal Processing*, vol. 37, pp. 984–995, July 1989.

[4] D. J. Farina, "Superresolution compact array radiolocation technology (SuperCART) project,", Flam & Russell Tech. Rep. 185, Nov. 1990.

[5] A. Nehorai and E. Paldi, "Superresolution compact array radiolocation technology (SuperCART) project," in *Asilomar Conf.*, 1991, pp. 566–572.

[6] G. F. Hatke, "Performance analysis of the superCART antenna array," MIT Lincoln Lab., Project Rep. #AST-22, Mar. 1992.

[7] A. J. van der Veen, P. B. Ober, and E. F. Deprettere, "Azimuth & Elevation computation in high resolution DOA estimation," *IEEE Trans. Signal Processing*, vol. 40, pp. 1828–1832, 1992.

[8] J. Li, "Direction and polarization estimation using arrays with small loops and short dipoles," *IEEE Trans. Antennas Propagat.*, vol. 41, pp. 379–387, Mar. 1993.

[9] G. F. Hatke, "Conditions for unambiguous source localization using polarization diverse arrays," in *27th Asilomar Conf.*, 1993, pp. 1365–1369.

[10] K. A. Burgess and B. D. Van Veen, "A subspace GLRT for vector-sensor array detection," in *IEEE Int. Conf. Acoust., Speech, Signal Processing*, vol. 4, 1994, pp. 253–256.

[11] ——, "Vector-sensor detection using a subspace GLRT," in *7th IEEE Statistical Signal Array Processing Workshop*, 1994, pp. 109–112.

[12] ——, "GLRT detection of broadband signals using an array of electromagnetic vector-sensors," in *28th Asilomar Conf.*, 1994, pp. 770–774.

[13] B. Hochwald and A. Nehorai, "Polarimetric modeling and parameter estimation with electromagnetic vector-sensors," in *IEEE Int. Geosci Remote Sensing Symp.*, vol. 2, 1994, pp. 1129–1132.

[14] A. Nehorai and E. Paldi, "Vector-sensor array processing for electromagnetic source localization," *IEEE Trans. Signal Processing*, vol. 42, pp. 376–398, Feb. 1994.

[15] B. Champagne, "Adaptive eigendecomposition of data covariance matrices based on first-order perturbations," *IEEE Trans. Signal Processing*, vol. 42, pp. 2758–2770, Oct. 1994.

[16] K.-C. Ho, K.-C. Tan, and W. Ser, "Investigation on number of signals whose directions-of-arrival are uniquely determinable with an electromagnetic vector-sensor," *Signal Processing*, vol. 47, no. 1, pp. 41–54, Nov. 1995.

[17] B. Hochwald and A. Nehorai, "Identifiability in array processing models with vector-sensor applications," *IEEE Trans. Signal Processing*, vol. 44, pp. 83–95, Jan. 1996.

[18] K.-C. Tan, K.-C. Ho, and A. Nehorai, "Uniqueness study of measurements obtainable with arrays of electromagnetic vector-sensors," *IEEE Trans. Signal Processing*, vol. 44, pp. 1036–1039, Apr. 1996.

[19] ——, "Linear independence of steering vectors of an electromagnetic vector-sensor," *IEEE Trans. Signal Processing*, vol. 44, pp. 3099–3107, Dec. 1996.

[20] K. T. Wong and M. D. Zoltowski, "High accuracy 2-D angle estimation with extended aperture vector-sensor array," in *IEEE Int. Conf. Acoust., Speech, Signal Processing*, vol. 5, 1996, pp. 2789–2792.

[21] ——, "Uni-vector-sensor ESPRIT for multi-source azimuth, elevation, and polarization estimation," *IEEE Trans. Antennas Propagat.*, vol. 45, pp. 1467–1474, Oct. 1997.

[22] M. D. Zoltowski and K. T. Wong, "Extended-aperture spatial diversity & polarization diversity using a sparse array of electric dipoles or magnetic loops," in *IEEE Int. Veh. Technol. Conf.*, 1997, pp. 1163–1167.

[23] K. T. Wong and M. D. Zoltowski, "Closed-form underwater acoustic direction finding with arbitrarily spaced vector-hydrophones at unknown locations," in *IEEE Int. Symp. Circuits Syst.*, vol. 4, 1997, pp. 2557–2560.

[24] ——, "Polarization-beamspace self-initiating MUSIC for azimuth/elevation angle estimation," in *Inst. Elect. Eng. Radar'97 Conf.*, 1997, IEE Conference Publication, pp. 328–333.

[25] K. T. Wong, "Adaptive geolocation and blind beamforming for wideband fast frequency-hop signals of unknown hop sequences and unknown arrival angles using an electromagnetic vector-sensor," in *IEEE Int. Conf. Commun.*, vol. 2, 1998, pp. 758–762.

[26] K. T. Wong and M. D. Zoltowski, "Closed-form direction finding with arbitrarily spaced electromagnetic vector-sensors at unknown locations," in *IEEE Int. Conf. Acoust., Speech, Signal Processing*, vol. 4, 1998, pp. 1949–1952.

[27] K. T. Wong, "Geolocation for partially polarized electromagnetic sources using multiple sparsely and uniformly spaced spatially stretched vector-sensors," in *IEEE Int. Conf. Circuits Syst.*, vol. 3, 1999, pp. 170–174.

[28] ——, "A novel closed-form azimuth/elevation angle and polarization estimation technique using only electric dipole triads or only magnetic loop triads with arbitrary unknown spacings," in *IEEE Int. Conf. Circuits Syst.*, vol. 3, 1999, pp. 207–210.

[29] K.-C. Ho, K. C. Tan, and B. T. G. Tan, "Estimation direction-of-arrival of partially polarized signals with electromagnetic vector senors," *IEEE Trans. Signal Processing*, vol. 47, pp. 2845–2852, Oct. 1999.

[30] A. Nehorai and P. Tichavsky, "Cross-product algorithms for source tracking using an EM vector-sensor," *IEEE Trans. Signal Processing*, vol. 47, pp. 2863–2867, Oct. 1999.

[31] M. D. Zoltowski and K. T. Wong, "ESPRIT-based 2-D direction finding with a sparse uniform array of electromagnetic vector-senors," IEEE Trans. Signal Processing, to be published.

[32] ——, "Closed-form eigenstructure-based direction finding using arbitrary but indenical subarrays on the sparse uniform Cartesian array grid," IEEE Trans. Signal Processing, to be published.

Kainam Thomas Wong (S'85–M'97) received the B.S.E. (chemical engineering) degree from University of California, Los Angeles (UCLA), in 1985, the B.S.E.E. degree from the University of Colorado, Boulder, in 1987, the M.S.E.E. degree from the Michigan State University, East Lansing, in 1990, and the Ph.D. degree in electrical engineering from Purdue University, West Lafayette, IN, in 1996.

He was a Manufacturing Engineer at the General Motors Technical Center, Warren, MI, from 1990 to 1991, a Senior Professional Staff Member at the Johns Hopkins University Applied Physics Laboratory, Laurel, MD, from 1996 to 1998, an Assistant Professor at Nanyang Technological University, Singapore, in 1998, and since 1998 has been an Assistant Professor in the Department of Electronic Engineering, Chinese University of Hong Kong. He is a contributing author to about 70 articles for the telecommunications section of the inaugural edition of the *CRC Dictionary of Pure and Applied Physics* and the *CRC Comprehensive Dictionary of Physics*. His current research interests are in signal processing for communications and sensor array signal processing.

Dr. Wong serves on the Technical Program Committees of the 1999 and 2000 IEEE Wireless Communications and Networking Conference (WCNC'99 and WCNC'00), the 1999 IEEE International Workshop on Intelligent Signal Processing and Communication Systems (ISPACS'99), the EuroComm 2000 Conference, and the 2000 Spring IEEE Vehicular Technology Conference (VTCI'00 Spring). He also serves on the Organizing Committees of the 2000 IEEE International Symposium on Circuits and Systems (ISCAS'00) and the Symposium 2000 on Adaptive Signal Processing, Communications and Control (AS-SPCC).

Michael D. Zoltowski (S'80–M'86–SM'95–F'99) was born in Philadelphia, PA, on August 12, 1960. He received both the B.S. and M.S. degrees in electrical engineering (highest honors) from Drexel University, in 1983, and the Ph.D. degree in systems engineering from the University of Pennsylvania, in 1986, both located in Philadelphia, PA.

From 1982 to 1986, he was an Officer and Naval Research Graduate Fellow. In 1986 he joined the faculty of Purdue University, West Lafayette, IN, where he currently holds the position of Professor of electrical and computer engineering. During 1987 he held a position of Summer Faculty Research Fellow at the Naval Ocean Systems Center, San Diego, CA. He is a contributing author to *Adaptive Radar Detection and Estimation* (New York: Wiley, 1991), *Advances in Spectrum Analysis and Array Processing, Vol. III* (Englewood Cliffs, NJ: Prentice-Hall, 1994), and the *CRC Handbook on Digital Signal Processing* (Boca Raton, FL: CRC, 1996). He has served as a Consultant to the General Electric Company. His present research interests include space–time adaptive processing and blind antenna array beamforming for all areas of mobile and wireless communications, radar, and global positioning systems.

Dr. Zoltowski was the recipient of the IEEE Signal Processing Society's 1991 Paper Award (*Statistical Signal and Array Processing Technical Area*). He was the recipient of the IEEE Outstanding Branch Counselor Award for 1989–1990 and the Ruth and Joel Spira Outstanding Teacher Award for 1990–1991. He was an associate editor for the IEEE TRANSACTIONS ON SIGNAL PROCESSING and is presently an Associate Editor for the IEEE COMMUNICATIONS LETTERS. Within the IEEE Signal Processing Society, he is a member of the Technical Committee for the Statistical Signal and Array Processing Area and a member of the Education Committee.